Amikacin Combined with Fosfomycin for Treatment of Neonatal Sepsis in the Setting of Highly Prevalent Antimicrobial Resistance

Christopher A Darlow[a]#, Fernando Docobo-Perez[b], Nicola Farrington[a], Adam Johnson[a], Laura McEntee[a], Jennifer Unsworth[a], Ana Jimenez-Valverde[a], Silke Gastine[c], Ruwanthi Kolamunnage Dona[d], Renata M A de Costa[e], Sally Ellis[e], François Franceschi[e], Joseph F Standing[c], Mike Sharland[f], Michael Neely[g], Laura Piddock[e,h], Shampa Das[a], William Hope[a]

[a] Antimicrobial Pharmacodynamics and Therapeutics, University of Liverpool, Liverpool Health Partners, UK

[b] Departamento de Microbiología, Universidad de Sevilla, Sevilla, Spain

[c] Great Ormond Street Institute of Child Health, University College London, London, UK.

[d] Department of Health Data Science, University of Liverpool, Liverpool Health Partners, UK

[e] Global Antibiotic Research and Development Partnership, 15 Chemin Louis-Dunant, 1202 Geneva, Switzerland

[f] Paediatric Infectious Diseases Research Group, St George's University of London, UK

[g] Children's Hospital Los Angeles and the Keck School of Medicine, University of Southern California, Los Angeles, CA, USA

[h] Antimicrobials Research Group, School of Immunity and Infection, Institute for Microbiology and Infection, University of Birmingham, UK

20

21 Running head: Amikacin and fosfomycin combination pharmacodynamics

22

23 # Address correspondence to Christopher A. Darlow, cdarlow@liverpool.ac.uk

ABSTRACT

Antimicrobial resistance (particularly by extended spectrum β-lactamase and aminoglycoside modifying enzyme production) in neonatal sepsis is a significant global problem, particularly in low- and middle-income countries, causing an estimated 430,000-680,000 deaths annually. High rates of resistance are reported for the current WHO-recommended first-line antibiotic regimen for neonatal sepsis; ampicillin and gentamicin. We assessed the utility of fosfomycin and amikacin as a potential alternative regimen to be used in settings of increasingly prevalent antimicrobial resistance.

The combination was studied in a 16 arm dose ranged hollow-fiber infection model (HFIM) experiment. The presence of amikacin or fosfomycin enhanced bactericidal activity and prevented emergence of resistance compared to monotherapy of either antibiotic. Modelling of the experimental quantitative outputs and data from checkerboard assays, indicated synergy.

We further assessed the combination regimen at clinically relevant doses in HFIM with nine Enterobacterales strains with high fosfomycin/amikacin MICs and demonstrated successful kill to sterilisation in 6/9 strains. From these data, we propose a novel combination breakpoint threshold for microbiological success for this antimicrobial combination against Enterobacterales - MIC_F * MIC_A < 256 (where MIC_F and MIC_A are MICs for fosfomycin and amikacin). Monte Carlo simulations predict that a standard fosfomycin/amikacin neonatal regimen will achieve a >99% probability of pharmacodynamic success for strains with MICs below this threshold.

We conclude that the combination of fosfomycin with amikacin is a viable regimen for the empiric treatment of neonatal sepsis and is suitable for further clinical assessment in a randomised controlled trial.

Introduction

Neonatal sepsis is a common condition with a high mortality (1). Leading causative pathogens are both Gram-negative (e.g. *E. coli*, *K. pneumoniae*) and Gram-positive organisms (e.g. *Staphylococcus aureus, Streptococcus agalactiae* (Group B streptococci - GBS)) (1). Neonatal sepsis accounts for an estimated 430,000 - 680,000 deaths annually, with the highest mortality in low- and middle-income countries (LMICs) (2, 3). The World Health Organisation (WHO) currently recommends a narrow-spectrum β-lactam agent (e.g. amoxicillin or penicillin G) in combination with gentamicin as the first line empiric regimen to treat neonatal sepsis (4, 5). This regimen has an acceptable safety profile, is active against common causative wild-type organisms, is inexpensive and feasible to administer. However, clinical efficacy is increasingly compromised by the rise of antimicrobial resistance (AMR).

Multiple epidemiological studies of neonatal sepsis demonstrate significant levels of drug resistance, particularly to β-lactams and gentamicin (6–12), with a variety of increasingly prevalent resistance mechanisms such as extended spectrum β-lactamases (ESBLs) and aminoglycoside modifying enzymes (AMEs). In hospital settings, resistance rates of Gram-negative bacteria causing neonatal sepsis to amoxicillin and gentamicin are approximately 80% and 60%, respectively, with some regional variation (6–12). Alternative options are urgently required for the treatment of neonatal sepsis caused by multi- and extremely-drug resistant (MDR and XDR) bacteria and suitable for use in LMIC settings.

A potential replacement regimen would need to provide spectrum of activity against the commonly encountered pathogens and resistance motifs. Additionally, if the regimen were a

69 combination of two agents, a favourable pharmacodynamic interaction would required.
70 Antimicrobial interactions can be defined by several metrics and definitions (13). However, the
71 interaction model described by Greco based on Loewe additivity (14, 15) allows determination
72 and quantification of any interaction with precision and without arbitrary thresholds for
73 determining the natures of interaction. Conceptually, this can be understod as follows; the
74 effect of two agents in combination can be described as Total Drug Effect = A + B + C, where A
75 and B are the effects of each drug alone, and C is the additional effect of the two agents in
76 combination. A value of C > 0 indicates synergy; C is negative, the agents are antagonistic; and if
77 C = 0 the agents have no interaction and the effects of the two drugs are additive only.

78 Amikacin and fosfomycin have several attributes that make them potential candidates for use
79 in neonatal sepsis. They are off-patent with a neonatal licence, have an acceptable safety
80 profile with limited toxicities (16, 17), and have efficacy against commonly encountered
81 multidrug resistant (MDR) pathogens. We therefore studied the potential utility of this
82 combination for neonatal sepsis by assessing *in vitro* activity, the nature and extent of any
83 pharmacodynamic interaction using checkerboard assays and hollow fiber infection models
84 (HFIMs), and defined candidate combination regimens suitable for further clinical study.

Results

In vitro susceptibility testing

A panel of 40 strains of bacterial species was assembled to give a representative range of bacteria that cause neonatal sepsis in a LMIC setting, with a majority of strains harbouring relevant resistance motifs for geographic regions of interest. These include 10 methicillin-resistant *Staphyloccocus aureus* (MRSA) strains, 10 *E. coli* and 10 *K. pneumoniae* strains (all ESBL or carbapenemase producers), and 10 wild-type *S. agalactiae* strains (Table S1). The MIC distributions for fosfomycin and amikacin against this panel of strains are shown in Table 1. The modal amikacin MIC was 2-4 mg/L (excluding the intrinsically resistant *S. agalactiae*, inhibited by a modal MIC of >32 mg/L); the modal fosfomycin MIC was 2 mg/L (excluding the *K. pneumoniae* strains, which have a modal MIC of >32mg/L, likely due to a high incidence of chromosomal FosA (18)).

In vitro drug-drug interaction modelling

Checkerboard assays were performed on a selection of the neonatal sepsis panel strains (n=16). These strains were selected on the basis of having MICs >0.0625mg/L and <32mg/L for fosfomycin and amikacin. An interaction model originally developed by Greco (14) was fitted to the dataset to estimate a pharmacodynamic interaction parameter, α, for each strain (Fig. 1). A value of α for the interaction of two agents is interpreted as follows: a lower bound of the 95% CI of $\alpha > 0$ indicates a synergistic interaction; an upper bound of the 95% CI of $\alpha < 0$ indicates an antagonistic interaction; a 95% CI crossing 0 indicates no evidence of interaction i.e. simple

additivity (14)). A total of 9/16 individual strains had CIs >0 (and therefore indicated synergy); the remaining 7/16 strains had CIs crossing 0 (and therefore demonstrated no evidence of interaction). When the α value output of the models fitted to each strains were combined in a meta-analysis, the combined α interaction value was 0.1705 (95% CI 0.0811 to 0.2599), with low inter-strain heterogeneity (I^2 = 30.7%, p value = 0.383) indicating a synergistic effect observed across all species/strains tested.

Pharmacodynamic interaction of fosfomycin and amikacin using neonatal PK

To determine the nature and magnitude of the pharmacodynamic interaction between fosfomycin and amikacin using neonatal concentration-time profiles, a hollow fiber infection model (HFIM) was used (Fig. 2) using the *E coli* ST195 strain, a CTX-M-14 producer from Laos (amikacin MIC 4 mg/L; fosfomycin MIC 1 mg/L) (19) . These experiments were conducted following preliminary dose-finding experiments with each drug alone to define informative parts of the drug exposure-response and drug exposure-emergence of resistance relationships. For fosfomycin, the EC_{20}, EC_{50}, and EC_{80} for bactericidal effect were achieved with $fAUC_{0\text{-}24}$ of 25, 200 and 400 mg*h/L, respectively. For amikacin, the EC_{20}, EC_{50}, and EC_{80} were achieved with $fAUC_{0\text{-}24}$ of 50, 200 and 380 mg*h/L, respectively.

The pharmacodynamics of the fosfomycin-amikacin combination was determined in a 16-arm 4x4 experiment that included no-treatment controls, each drug alone at the three doses, and an interaction matrix of all 2-drug dose combinations as shown in Fig. 3. When administered alone, increasing fosfomycin exposures resulted in profound early bacterial killing. However,

failure to achieve sterility led to rapid regrowth, with emergence of a resistant clone(s) with fosfomycin MICs of ≥128mg/L, with maximal emergent resistance at $fAUC_{0\text{-}24}$ of 50 and 200 mg*h/L (Fig. 3, Panels 1-4). Similarly, progressively increasing exposures of amikacin as monotherapy led to initial suppression of logarithmic growth with subsequent exposure-dependent emergence of a resistant subpopulation with amikacin MICs ≥16mg/L, with maximal emergent resistance at $fAUC_{0\text{-}24}$ of 380 mg*h/L (Fig. 3, Panels 1,5, 9, & 13).

In combination, fosfomycin and amikacin achieved a greater magnitude of initial bacterial kill, with delayed and reduced emergence of resistance to fosfomycin and amikacin, compared with equivalent drug exposures in monotherapy. Higher combination exposures achieved sterility. The relationship between drug exposure and the emergence of resistance with each drug administered alone formed an 'inverted U' (20). Fosfomycin and amikacin in combination resulted in the suppression of resistance that failed to do so at comparable drug exposures in monotherapy of each drug (Fig. 3, Panels 11,12 & 14-16). As the exposure of the other antibiotic increased, the 'inverted U' shifted to the left as emergence of resistance was progressively suppressed (Fig. 4).

The nature and magnitude of the pharmacodynamic interaction between fosfomycin and amikacin was estimated by fitting a pharmacodynamic interaction model to the PK-PD data (Table 2). The R-squared values for the observered vs individual predicted values were 0.875 (free fosfomycin concentrations), 0.963 (free amikacin concentrations), 0.869 (total bacterial count), 0.944 (fosfomycin-resistant bacterial count) and 0.669 (amikacin-resistant bacterial count). There were synergistic relationships for the effects of the combination on susceptible, fosfomycin-resistant, and amikacin-resistant bacteria with α values of 13.046 [95% CI 0.761 –

25.331], 20.520 [95% CI 11.727 – 29.313], and 25.227 [95% CI 14.485 – 35.969], respectively. Hence, the combination of fosfomycin and amikacin was synergistic in terms of killing both drug-susceptible and -resistant subpopulations.

Assessment of a Neonatal Combination Regimen of Fosfomycin and Amikacin

We assessed the pharmacodynamics of the combination of fosfomycin and amikacin using neonatal concentration-time profiles of each drug over a 7 day period. For amikacin, we used a humanised neonatal dose of 15 mg/kg q24h (21) and a median neonatal half-life of 7 hr (22). For fosfomycin we used a humanised neonatal dose of 100mg/kg q12h with a half-life of 5.2 hr, based on preliminary data from the NeoFosfo trial (23). We selected nine Gram-negative bacteria as the challenge strains that had a range of MICs to both drugs and had different mechanisms of resistance (Table 3). We successfully recapitulated the target free drug PK profiles associated with each regimen (data not shown).

The summary pharmacodynamics are shown in Fig. 5 (full pharmacodynamic output are shown in Fig. S1-9). When administered alone, amikacin and fosfomycin failed to achieve extinction in 9/9 and 7/9 strains, respectively. All arms with strains inhibited by fosfomycin MICs >4mg/L treated with fosfomycin monotherapy had rapid emergence of resistance within 24h. The three strains inhibited by fosfomycin MICs $\leq$4mg/L were either killed to sterility (two strains) or had delayed emergence of resistance towards the end of the experiment. In contrast, the combination regimen achieved extinction in 6/9 strains. The strains for which the combination failed were all inhibited by MICs $\geq$ 32mg/L and $\geq$ 8mg/L for fosfomycin and amikacin,

respectively. The distribution of combined fosfomycin and amikacin MICs versus response is shown in Fig. 5a. In this figure, a plane (or line) delineated two groups of strains, defined by the fosfomycin/amikacin MICs, that predicted success (defined as sterility at the end of the experiment) and failure. This 'breakpoint plane' was described in the following Cartesian format $MIC_A * MIC_F = 256$, where MIC_A and MIC_F are amikacin and fosfomycin MICs, respectively. In a clinical context, this means that if the product of the amikacin and fosfomycin MICs inhibiting a bacterial pathogen is < 256, then treatment with a neonatal regimen of fosfomycin and amikacin in combination can be predicted to succeed (i.e. the bacterium is 'sensitive' to this combination).

The amikacin/fosfomycin combination success data can also be arranged according to the *f*AUC:MIC ratio for each drug, as shown in Fig. 5b, with a similar plane describing the threshold for successful treatment with the combination. This target plane can be described with the form $(fAUC_F / MIC_F) * (fAUC_A / MIC_A) = 2709.5$ (where F and A subscripts denote fosfomycin and amikacin *f*AUCs and MICs respectively). Interpreted in a clinical context, if the product of the amikacin and fosfomycin *f*AUC:MIC ratios is >2709.5, then the target for pharmacodynamic success has been met, with predicted treatment success.

Monte Carlo Simulations

Amikacin and fosfomycin *f*AUCs for 10,000 neonates were created using a Monte Carlo simulation from a neonatal fosfomycin model that included neonatal covariate distributions based on a neonatal cohorts from the NeoFosfo trial and a recently completed global neonatal

sepsis observational study (NeoOBS) (23, 24) and a recently published neonatal amikacin model (25). Simulated dosing regimes were fosfomycin 100mg/kg q12 for neonates ≤7 days old and 150mg/kg q12 for neonates >7 days, as suggested by the NeoFosfo trial results and the EMA dosing recommendations (23, 26). Simulated amikacin dosages were 15mg/kg q24 for all neonates > 2kg; neonates weighing ≤ 2kg were dosed at q48 if ≤7 days old and q36 if >7 days old (27).

Using the target relationships defined above, we calculated a combined probability of pharmacodyamic target attainment for both drugs across MIC ranges (1 – 256 mg/L) (Table 4). These simulated *f*AUCs demonstrated ≥99% predicted target attainment for Enterobacterales with amikacin and fosfomycin MICs below the 'breakpoint plane'. This indicates a high likelihood that fosfomycin and amikacin in combination at the simulated dosing regimens (i.e. at standard neonatal doses) will successfully treat neonatal sepsis caused by these pathogens.

Discussion

In both static and dynamic *in vitro* pharmacological models there was unequivocal synergistic interactions between amikacin and fosfomycin when measuring by bactericidal killing and the prevention of emergence of antimicrobial resistance. In particular, the addition of increasing doses of the second agents suppresses the 'inverted U' of antimicrobial resistance emergence (20) (Fig. 4) preventing the resistance observed at equivalent doses in monotherapy. These characteristics are unaffected by the presence of resistance mechanisms that render first line agents ineffective (e.g. ESBL and AMEs) in the bacteria tested in our experiments. The combination fosfomycin and amikacin is therefore a potentially useful regiment for empiric treatment of neonatal sepsis in the context of high prevalence of these resistance mechanisms

Prediction of antimicrobial success has traditionally been conceived using breakpoint thresholds on a scale of a single drug concentration, with the treatment success dependent upon the bacteria being inhibited by a MIC being above or below a certain threshold on this scale. Our data suggests that using conventional monotherapy breakpoints is of limited value in combination antibiotics (Fig. 5). Here, we propose a novel two-dimensional breakpoint concentration threshold for treatment success defined by the Cartesian function of the pathogen's fosfomycin and amikacin MIC; $MIC_A * MIC_F = 256$, where A and F subscripts denote amikacin and fosfomycin MICs respectively. Enterobacterales pathogens that are inhibited by amikacin and fosfomycin MICs lying beneath this threshold (i.e. $MIC_A * MIC_F < 256$) can be predicted to be successfully treated by the standard regimen of these agents used in neonates i.e. it is specific to a neonatal context.

In a further extension, we also propose a novel combination pharmacodynamic target threshold for the combination regimen for predicted treatment success, described in the following Cartersian format: $(fAUC_F / MIC_F) * (fAUC_A / MIC_A) = 2709.5$. The probabilities of standard neonatal regimens of these drugs attaining this threshold, for bacteria inhibited by a range of MIC combinations and incorporating the variability of neonatal drug exposure, are summarised in Table 4.

We aimed to ensure a diversity of resistance mechanisms across the strains used, with commonly encountered resistance motifs in LMICs represented, acknowledging we are limited to the nine strains used. Whilst it is possible that bacteria with resistance mechanisms not examined in our experiments do not follow the relationship described, we nevertheless believe that the pharmacodynamic relationship described above can be applied to bacterial pathogens using the phenotype alone (i.e. MIC), agnostic of the genotype, as for currently used breakpoint concentrations.

In our HFIM experiments the monotherapy arms failed with strains inhibited by fosfomycin and amikacin MICs below their EUCAST breakpoint concentrations (32mg/L for fosfomycin and 8mg/L for amikacin (28)). The underperformance of amikacin partially supports the recent downward revision of aminoglycoside breakpoint concentrations by EUCAST with a recommendation to avoid aminoglycoside monotherapy for systemic infections (28), but also reflects the observed greater tendency of aminoglycoside exposure to generate emergence of resistant small-colony variants *in vitro* than is observed *in vivo* (29). Failure of fosfomycin as monotherapy for strains inhibited by MICs >4mg/L supports suggestions that the breakpoint concentration for neonatal systemic infections should be lower than the currently stated

246 EUCAST breakpoint for adult systemic infections of 32mg/L (28) (as has previously also been
247 suggested in an adult context too (30)). However, the ideal breakpoint concentration for
248 fosfomycin alone is difficult to define because this agent should not be used as monotherapy
249 due to potential for rapid emergence of resistance (31, 32).

250 There is an increasing number of experimental models of neonatal infection and sepsis (33, 34).
251 HFIMs has been previously used to explore the pharmacodynamics of vancomycin and
252 teicoplanin for neonatal sepsis (33, 35). HFIM has the advantage of enabling the simulation of
253 neonatal pharmacokinetics to explore drug exposure effect and drug exposure resistance
254 relationships that are specific to this special population. This is extremely difficult to achieve in
255 laboratory animal models, due to inherent pharmacokinetic differences with humans.
256 Furthermore, laboratory animal models of bacteraemia have additional difficulties in
257 establishing pharmacodynamic relationships to due to the relatively low and intermittently
258 detectable bacterial densities. The HFIM overcomes these limitations.

259 However, the HFIM does not replicate the anatomical barriers that may be important for
260 infections of the lung and brain, and does not contain any immunological effectors (even if
261 these are immature in neonates) that may contribute to antimicrobial activity. Furthermore,
262 the relatively high density of the inoculum used in HFIM to ensure reproducible results (circa.
263 10^6 cfu/mL) is higher than the estimates for the bacterial density in the bloodstream of
264 neonates with sepsis (circa. 10^0-10^3 CFU/mL) (36, 37). For these reasons, the conclusions from
265 the HFIM may be conservative and represent a worst-case scenario for regimen identification.

266 Furthermore, the conclusions of these experiments are applicable only to the treatment of
267 systemic infections (i.e. neonatal sepsis) given the replication of neonatal systemic drug

exposures. Whilst both amikacin and fosfomycin have a degree of CSF penetration (amikacin has a CSF partition coefficient of 0.1 in neonates (38); fosfomycin has a CSF coefficient of 0.15-0.2 in adults (39), with neonatal data expected in the Neofosfo trial (23)), the CSF drug exposures and the behaviour of bacterial inoculums in neonatal meningitis will be significantly different to those modelled in this system. As such, we cannot comment on the adequacy of this regimen for neonatal meningitis.

Despite these limitations, we conclude these experiments demonstrate that the regimen of fosfomycin and amikacin in combination is synergistic in both bactericidal effect and prevention of acquired antimicrobial resistance to either drug, with a defined threshold for probable treatment success. Additionally both agents have attributes that make them suitable for use in LMIC settings: i) Stability at room temperature (40, 41); ii) Ease of administration with once or twice daily dosing; iii) Minimal toxicities; iv) Off-patent status, and therefore potential affordability; v) Potential activity, in combination, to the predominant bacterial causes of neonatal sepsis. We conclude that this combination regimen could be considered appropriate for empiric treatment of neonatal sepsis in LMIC settings, contingent on the following: i) epidemiological MIC distributions for both drugs favourably related to the proposed breakpoint threshold; and ii) a favourable assessment of efficacy and safety in a multi-centre neonatal sepsis clinical trial.

Methods and Materials

Antimicrobial agents. Amikacin (Alfa Aesar, Haverhill), and fosfomycin (Sigma-Aldrich, St Louis) were purchased. Both agents were stored at 2-8^{o}C in anhydrous form. Fresh solutions were prepared in sterile distilled water prior to any use. For the *in vitro* hollow fiber infection model (HFIM) experiments, a licensed pharamaceutical preparation of fosfomycin (Fomicyt, Kent Pharmaceuticals Ltd) were used and were prepared using sterile distilled water.

Media and agar. Cation-adjusted Muller Hinton broth (MHB) (Sigma-Aldrich, St Louis) was used as the primary media in all experiments. As fosfomycin requires the presence of glucose-6-phosphate (G6P) for bacterial cell entry (42) the MHB was supplemented with 25mg/L G6P (Sigma-Aldrich, St Louis) in experiments where fosfomycin is used. Mueller Hinton agar (MHA) was used in all agar plates. Commercially pre-prepared 20mL round MHA plates (Fisher Scientific, Waltham) or self-prepared 50ml square MHA plates (MHA from Sigma-Aldrich; square plates from VWR, Radnor) were used in all experiments. For drug-containing plates, MHA was supplemented with antibiotic (with 25mg/L G6P in the case of fosfomycin) and prepared within each antibiotic's stability limits. Drug concentrations in agar were four times the MIC of the specific bacterial strain used in a given experiment.

***Bacterial Isolates*.** Isolates were supplied by JMI, IHMA, Public Health England (PHE), LGC standards, University of Birmingham, University of Oxford, and Royal Liverpool University Hospital. For the initial non-dynamic *in vitro* experiments, a collection of strains was collated representing a range of common possible neonatal sepsis bacterial pathogens and resistance mechanisms in an AMR prevalent environment. In total, this included 10 strains of each of the following: Group B streptococci, methicillin resistant *Staphylococcus aureus* (MRSA), *Escherichia*

coli, and *Klebsiella pneumoniae*. All of the Gram-negative bacteria were extended spectrum β-lactamase (ESBL) (nine *E. coli* and nine *K. pneumoniae* strains*)* or carbapenemase producers (one *E. coli* and one *K. pneumoniae strain)*. Some of these strains were used in the HFIM based on their MICs, including a further two *K. pneumoniae* and one *E. coli* (ESBL producers) not included in the original 40 strain panel. (Full details of the isolates are detailed in Supplementary Data Table 1). All isolates were stored in glycerol at -80^{o}C and sub-cultured onto two MHA plates for 18-24h at 37^{o}C prior to each experiment. In each non-HFIM experiment, colonies were suspended in PBS to MacFarland standard 0.5 (1x10^{8} CFU/mL) and diluted to the target concentration. For HFIM experiments, bacteria was incubated in MHB until the bacteria entered exponential growth, and quantified by optical density (600nm) according to a strain specific standard growth curve.

***Antimicrobial susceptibility testing*.** Fosfomycin and amikacin minimum inhibitory concentrations (MICs) for the panel of representative neonatal sepsis bacterial pathogens were determined using the EUCAST broth microdilution methodology (43). *E. coli* ATCC 25922 or *S. aureus* ATCC 29213 were used as controls in all experiments. The antibiotic gradient strip assay method was used for isolates from the hollow fiber experiment. Briefly, an inoculum of the isolate was made using a suspension of a sweep of colonies into PBS to a McFarland standard of 0.5. A lawn of the inoculum was plated onto a MHA plate and an antibiotic gradient strip (Etest, Biomerieux, Marcy-l'Étoile, France) placed on the plate, which is subsequently incubated for 18-24h at 37^{o}C before reading. Interpretation of susceptibility was determined using 2020 EUCAST breakpoints (28). The breakpoint for IV fosfomycin was used for fosfomycin MIC interpretation.

***In vitro pharmacodynamic assays*.** Checkerboard assays were used on selected strains to assess the pharmacodynamic interaction of the fosfomycin/amikacin combination. Strains were selected based on having MICs $\leq$32mg/L and >0.0625 mg/L to both fosfomycin and amikacin. 100 μL of antimicrobials in sterile distilled water were added to the an 8x8 grid on a 96 well plate, with concentration gradients created with 1:2 serial dilutions along each axis, with the final row/column having 0 mg/L of the appropriate drug. The drug concentration range used on each plate was chosen according to the drug MICs of each strain, with the maximum concentration of each antimicrobial being 4x MIC for that strain. The inoculum was made up to $1x10^6$ CFU/mL in MHB and quantified using 1:10 serial dilution onto MHA plates. 100μl of the inoculum was added to each well of the prepared checkerboard. The well containing 0 mg/mL of each drug acted as the positive control; an additional row of blank MHB on the plate acted as negative control. Plates were incubated 18-24h at 37^{o}C before being read by optical densitometer (Varioskan, Thermo Fisher) at 600nm. Plates were considered valid if the MIC on the monotherapy rows of the checkerboard were within 1 dilution of previously determined MICs, the negative controls had no growth, and the prepared inoculum was within 6-14 x 10^5 CFU/mL.

Raw optical densitometer (OD) readings were normalised to that of the positive control. The readouts were then modelled using Greco's model of drug synergy (15) using ADAPT 5 (44), with determination of α, with confidence intervals calculated using standard error of the model outputs. Meta-analysis was performed on the output of the combination using the R package 'Metafor' (45).

Hollow Fiber Infection Model. The hollow fiber infection model (HFIM) is a well-established dynamic model stimulating the pharmacodynamic effect of antimicrobials with physiological dynamic concentrations (46). The HFIM method was used largely as described previously (33). Briefly, each arm in the HFIM is set up as demonstrated in Fig. 2; monotherapy arms omit the supplementary compartments. MHB is pumped into the central compartment at a rate set to simulate a physiological clearance rate for the drug, with all media in the central compartment above 300 mL removed via an elimination pump. The target simulated half-lives for fosfomycin and amikacin were 5.1 and 7 hours respectively. The neonatal half-life of fosfomycin was determined from then unpublished data from the NeoFosfo trial (23). The neonatal half-life of amikacin was sourced from the SPC (47) and confirmed with other published neonatal clinical PK data (48–52) To account for the difference in clearance between fosfomycin and amikacin, supplementary compartments were set up according the principles laid out by Blaser (53).

Throughout the HFIM experiments, inoculum concentrations were determined by serial dilution 1:10. A total of 10μL of each dilution was pipetted onto MHA plates; one drug-free and two containing either fosfomycin or amikacin. An additional 100μL of the original inoculum was plated onto a drug-free MHA plate to lower the limit of detection for total bacterial quantification (i.e. to 10 CFU/mL). Plates were then incubated at 37^{o}C for 18-24 hr for drug free plates, and 42-48 hr for drug-containing plates. After incubation, colonies were counted for at least two dilutions and the CFU/mL of the original inoculum was calculated.

Preliminary monotherapy experiments were performed with the ESBL-producing ST195 *E. coli* strain (fosfomycin MIC 1mg/L, amikacin MIC 4 mg/L; supplied by the University of Birmingham) (19). PK and PD outputs of these experiments were modelled using Pmetrics (54) and

parameters simulated using ADAPT (44) to determine the fosfomycin and amikacin doses required to achieve EC_{20}, EC_{50} and EC_{80} in terms of bactericidal effect within the HFIM. A 16-arm HFIM experiment was performed using a 4x4 dosing matrix using these three doses and no dose for both antibiotics in combination. The experiment was run over 96 hours, with a target initial inoculum of $1x10^6$ CFU/mL of ST195 inoculated into the hollow fiber cartridges. A dose of fosfomycin corresponding to the EC_{20}, EC_{50} and EC_{80} was administered every 12 hours to the primary central compartment only; an amikacin dose achieving the EC_{20}, EC_{50} and EC_{80} was administered to the primary and supplementary central compartments every 24 hours.

PK samples were taken for bioanalysis at four timepoints in dosing windows in days 1 and 3 of the experiment. Samples of inoculum were taken from each hollow fiber cartridge at 4 timepoints during the first 24h, then once daily before administration of dose until the 96h timepoint. Each sample was prepared and plated onto drug-free square agar plates and fosfomycin- and amikacin- containing plates, as described above. MICs from any viable colonies from each arm on the final timepoint were determined via antibiotic gradient strip assay .

Further HFIM experiments were performed assessing the effect of clinically relevant fosfomycin and amikacin doses leading to neonatal-like pharmacokinetic profile alone and in combination against a variety of bacteria with different fosfomycin and amikacin MICs. PK profiles of fosfomycin and amikacin were designed to have half-lives of 5.1 and 7 hours, with Cmax values of 250mg/L and 40mg/L respectively. These were determined from the sources used to determine the half-life, as described earlier. Nine parallel experiments were performed using nine Gram-negative strains with a wide distribution of fosfomycin and amikacin MICs (Table 3). Each individual experiment consisted of 4 arms; monotherapy arms for both fosfomycin and

amikacin, a combination therapy arm, and an untreated control. As this experiment aimed to replicate clinically relevant drug exposures in neonates, each experiment lasted 7 days to reflect the typical treatment course of neonatal sepsis. Four PK samples were taken in each of three dose intervals distributed evenly throughout the experiment. Four inoculum samples were taken on day 1, and once every 24h thereafter. These samples were quantified on drug-free, fosfomycin-, and amikacin-containing square MHA plates. MICs from any viable colonies from each arm on the final timepoint were determined via antibiotic gradient strip assay.

Amikacin Bioanalysis. The internal standard, [$^{2}H_{5}$] amikacin (Alsachim, Illkirch-Graffenstaden, France) was prepared in acetonitrile plus 5% trichloroacetic acid (TCA) (25 mg/L, Fisher Scientific, UK) and 150 μL was added to a 96-well protein precipitation plate (Phenomenex, Cheshire, UK). Fifty μL each of samples, blanks, calibrators in the range 0.5 – 50 mg/L and quality controls (0.75, 7.5 and 37.5 mg/L) were mixed with the internal standard on an orbital shaker. Liquid was drawn through the protein precipitation plate into a collection plate using a positive pressure manifold. Samples were evaporated under nitrogen (40 L/min) followed by reconstitution in water (Fisher Scientific, UK) and 0.1% heptafluorobutyric acid [Sigma-Aldrich, UK] and mixed using an orbital shaker prior to analysis by LC-MS-MS.

LC-MS-MS analysis was performed using an Agilent 1290 Infinity HPLC coupled to an Agilent 6420 triple quadrupole mass spectrometer fitted with an electrospray source controlled using Agilent MassHunter Data Acquisition software (Ver B.06.00). Analytes were injected (5 μL) onto a Discovery® HS C18 HPLC Column (2.1 mm x 50 mm, 3 μm, 50°C) and separated over a 3.5 min. gradient using a mixture of solvents A (LC-MS grade water with 0.1% (v/v) heptafluorobutyric acid) and B (HPLC grade acetonitrile with 0.1% (v/v) heptafluorobutyric acid). Separations were

performed by applying a linear gradient of 2% to 98% solvent B over 3 mins at 0.5 mL/min followed by an equilibration step (0.5 mins at 2% solvent B).

The mass spectrometer was operated in positive ion mode using a Multiple Reaction Monitoring (MRM) method with the specified mass transitions and collision energies: amikacin 586.4 > 163.2 (Ce 30 ev) and [$^{2}H_{5}$] amikacin 591.3 > 163.2 (Ce 30 ev). Mass spectrometry readouts were processed using Agilent Mass Hunter Quantitative Analysis (Ver B.05.02).

Prior to sample analysis, the analytical method was validated to assess recovery and matrix effects, inter- and intra-day accuracy and precision, carryover, dilution integrity, stability in matrix (4 hours at room temperature and 3 freeze thaw cycles) and processed sample stability (reinjection of extracts after 24hrs). The average recovery from matrix was 75.3%. The limit of quantification (LLQ) was defined as 0.5 mg/L and the limit of detection (LOD) 0.25 mg/L. The inter- and intra-day %CV on the three QC levels ranged from 2.5% – 5.7% and 2.9% – 6.41% respectively. The analyte was found to be stable in all conditions described above.

Fosfomycin Bioanalysis. The internal standard, Ethyl Phosphonic acid (Sigma Aldrich, UK) was prepared in acetonitrile (5 mg/L, Fisher Scientific UK) and 200 μL was added to a 96-well protein precipitation plate (Phenomenex, Cheshire, UK). Fifty μL each of samples, blanks, calibrators in the range 1 – 500 mg/L and quality controls (3.5, 35 and 350 mg/L) were mixed with the internal standard on an orbital shaker. Liquid was drawn through the protein precipitation plate into a collection plate using a positive pressure manifold with water and 2mM Ammonium acetate (150 μL) added to each well, before sealing and mixing on an orbital shaker.

LC-MS-MS analysis was carried out using the same technical setup as described above. Analytes were injected (5 μL) onto an Agilent ZORBAX RRHD HILIC Plus 95Å Column (2.1 mm x 50 mm, 1.8 μm, 40°C) and separated over a 3.5 min. gradient using a mixture of solvents A (LC-MS grade water with 2mM (v/v) ammonium acetate) and B (HPLC grade acetonitrile). Separations were performed by applying a linear gradient of 100% to 0% solvent B over 2 mins at 0.4 mL/min followed by an equilibration step (1.5 mins at 100% solvent B).

The mass spectrometer was operated in negative ion mode using a Multiple Reaction Monitoring (MRM) method with the specified mass transitions and collision energies: fosfomycin 137.1 > 79.0 (Ce 20 ev) and EPA 109.1 > 79.0 (Ce 20 ev). Mass spectrometry readouts were processed as described above.

This fosfomycin analytical method underwent the same validation process as the amikacin method described above. The average recovery from matrix was 80.9%. The LLQ was defined as 1 mg/L and the LOD 0.5 mg/L. The inter and intra day %CV on the three QC levels ranged from 6.5% – 8.1% and 4.7% – 6.9% respectively. The analyte was found to be stable in all conditions described above.

Modelling. Population PK models were constructed using the pharmacokinetic and pharmacodynamic outputs of the hollow fiber experiments using the population PK program Pmetrics using a nonparametric adaptive grid NPAG estimation routine (54). The structural model was based on Greco's models of pharmacological synergy (15) (described in full in Appendix 1).

Monte Carlo Simulation. A neonatal model for fosfomycin developed from the Neofosfo trial (23, 55) and previously published neonatal amikacin (56) was used to simulate fosfomycin/amikacin PK profiles from 10,000 neonates the linPK package in R (https://cran.r-project.org/web/packages/linpk/index.html). The simulated population was based on the demographic distribution of neonates in the Neofosfo trial (23) combined with data from an international multi-centre neonatal observational trial (24). From the simulated PK profiles, individual $fAUC_{0\text{-}24h}$ values were calculated from the first 24h.

Data availability: The programs ADAPT and Pmetrics are pubically available, with instructions, at https://bmsr.usc.edu/software/adapt/ and http://www.lapk.org/pmetrics.php respectively.

Acknowledgements: This work was funded the Global Antibiotic Research and Development Partnership (GARDP). GARDP was funded by the German Federal Ministry of Education and Research, German Federal Ministry of Health, Médecins Sans Frontières, Netherlands Ministry of Health, Welfare and Sport, United Kingdom Department for International Development, and the United Kingdom National Institute of Health Research. CD is also funded by the UK Medical Research Council (MR/N025989/1). The funders had no role in study design, data collection and interpretation, or the decision to submit the work for publication.

The authors thank Sam Lipworth for identifying and supplying the strains from the University of Oxford, Jonathan Folb for supplying GBS strains from the Royal Liverpool Hospital, and JMI and IMHA for gifting their strains for this work.

Declared Interest: None

476 **References**

477 1. Shane AL, Sánchez PJ, Stoll BJ. 2017. Neonatal sepsis. Lancet (London, England)
478 390:1770–1780.

479 2. Oza S, Lawn JE, Hogan DR, Mathers C, Cousens SN. 2015. Neonatal cause-of-death
480 estimates for the early and late neonatal periods for 194 countries: 2000-2013. Bull
481 World Health Organ 93:19–28.

482 3. Seale AC, Blencowe H, Manu AA, Nair H, Bahl R, Qazi SA, Zaidi AK, Berkley JA, Cousens
483 SN, Lawn JE, Agustian D, Althabe F, Azziz-Baumgartner E, Baqui AH, Bausch DG, Belizan
484 JM, Qar Bhutta Z, Black RE, Broor S, Bruce N, Buekens P, Campbell H, Carlo WA, Chomba
485 E, Costello A, Derman RJ, Dherani M, El-Arifeen S, Engmann C, Esamai F, Ganatra H,
486 Garcés A, Gessner BD, Gill C, Goldenberg RL, Goudar SS, Hambidge KM, Hamer DH,
487 Hansen NI, Hibberd PL, Khanal S, Kirkwood B, Kosgei P, Koso-Thomas M, Liechty EA,
488 McClure EM, Mitra D, Mturi N, Mullany LC, Newton CR, Nosten F, Parveen S, Patel A,
489 Romero C, Saville N, Semrau K, Simões EAF, Soofi S, Stoll BJ, Sunder S, Syed S, Tielsch JM,
490 Tinoco YO, Turner C, Vergnano S. 2014. Estimates of possible severe bacterial infection in
491 neonates in sub-Saharan Africa, south Asia, and Latin America for 2012: A systematic
492 review and meta-analysis. Lancet Infect Dis 14:731–741.

493 4. Fuchs A, Bielicki J, Mathur S, Sharland M, Van JN, Anker D. 2016. Antibiotic Use for Sepsis
494 in Neonates and Children: 2016 Evidence Update. WHO-Reviews 7.

495 5. World Health Organization. 2013. Pocket book of hospital care for childrenSecond Edi.
496 World Health Organisation, Geneva.

6. DeNIS collaboration. 2016. Characterisation and antimicrobial resistance of sepsis pathogens in neonates born in tertiary care centres in Delhi, India: a cohort study. Lancet Glob Heal 4:e752–e760.

7. Labi AK, Obeng-Nkrumah N, Bjerrum S, Enweronu-Laryea C, Newman MJ. 2016. Neonatal bloodstream infections in a Ghanaian Tertiary Hospital: Are the current antibiotic recommendations adequate? BMC Infect Dis 16.

8. Bandyopadhyay T, Kumar A, Saili A, Randhawa VS. 2018. Distribution, antimicrobial resistance and predictors of mortality in neonatal sepsis. J Neonatal Perinatal Med 11:145–153.

9. Jajoo M, Manchanda V, Chaurasia S, Jeeva Sankar M, Gautam H, Agarwal R, Yadav CP, Aggarwal KC, Chellani H, Ramji S, Deb M, Gaind R, Kumar S, Arya S, Sreenivas V, Kapil A, Mathur P, Rasaily R, Deorari AK, Paul VK. 2018. Alarming rates of antimicrobial resistance and fungal sepsis in outborn neonates in North India. PLoS One 13:1–16.

10. Yadav NS, Sharma S, Chaudhary DK, Panthi P, Pokhrel P, Shrestha A, Mandal PK. 2018. Bacteriological profile of neonatal sepsis and antibiotic susceptibility pattern of isolates admitted at Kanti Children's Hospital, Kathmandu, Nepal. BMC Res Notes 11:1–6.

11. Pokhrel B, Koirala T, Shah G, Joshi S, Baral P. 2018. Bacteriological profile and antibiotic susceptibility of neonatal sepsis in neonatal intensive care unit of a tertiary hospital in Nepal. BMC Pediatr 18:1–8.

12. Chaurasia S, Sivanandan S, Agarwal R, Ellis S, Sharland M, Sankar MJ. 2019. Neonatal sepsis in South Asia: Huge burden and spiralling antimicrobial resistance. BMJ. BMJ

518 Publishing Group.

519 13. Doern CD. 2014. When Does 2 Plus 2 Equal 5? A Review of Antimicrobial Synergy Testing
520 Downloaded from. 4124 jcm.asm.org J Clin Microbiol 52:4124–4128.

521 14. Greco WR, Bravo G, Parsons JC. 1995. The search for synergy: A critical review from a
522 response surface perspective. Pharmacol Rev. Pharmacol Rev.

523 15. Greco WR, Park HS, Rustum YM. 1990. Application of a New Approach for the
524 Quantitation of Drug Synergism to the Combination of cis -Diamminedichloroplatinum
525 and 1- β -d-Arabinofuranosylcytosine Application of a New Approach for the Quantitation
526 of Drug Synergism to the Combination of m-Diam. Cancer Res 50:5318–5327.

527 16. Iarikov D, Wassel R, Farley J, Nambiar S. 2015. Adverse Events Associated with
528 Fosfomycin Use: Review of the Literature and Analyses of the FDA Adverse Event
529 Reporting System Database. Infect Dis Ther 4:433–458.

530 17. Kent A, Turner MA, Sharland M, Heath PT. 2014. Aminoglycoside toxicity in neonates:
531 something to worry about? Expert Rev Anti Infect Ther 12:319–331.

532 18. Ito R, Mustapha MM, Tomich AD, Callaghan JD, McElheny CL, Mettus RT, Shanks RMQ,
533 Sluis-Cremer N, Doi Y. 2017. Widespread fosfomycin resistance in gram-negative bacteria
534 attributable to the chromosomal *fosA* gene. MBio 8:1–9.

535 19. Anu K, Esther K, Dunn Steven J, Dance David AB, Newton Paul N, Davong V, Sointu M,
536 Pakkanen Sari H, Andreas N, Cristoph H, Ann S, Teemu K, Jukka C, Alan M. 2019. Real-
537 time sampling of travelers shows intestinal colonization by multidrug-resistant bacteria
538 to be a dynamic process with multiple transient acquisitions. bioRxiv. bioRxiv.

20. Tam VH, Louie A, Deziel MR, Liu W, Drusano GL. 2007. The relationship between quinolone exposures and resistance amplification is characterized by an inverted U: A new paradigm for optimizing pharmacodynamics to counterselect resistance. Antimicrob Agents Chemother 51:744–747.

21. Joint Formulary Committee. British National Formulary (online). BMJ Gr ad Pharmacetucial Press.

22. Howard JB, McCracken GH, Trujillo H, Mohs E. 1976. Amikacin in newborn infants: comparative pharmacology with kanamycin and clinical efficacy in 45 neonates with bacterial diseases. Antimicrob Agents Chemother 10:205–210.

23. 2019. Intravenous and Oral Fosfomycin in Hospitalised Neonates With Clinical Sepsis (NeoFosfo) - NCT03453177. Clinicaltrials.gov.

24. 2018. NeoAMR Observational Study in Neonatal Sepsis - NCT03721302. ClinicalTrials.gov.

25. Illamola SM, Sherwin CM, van Hasselt JGC. 2018. Clinical Pharmacokinetics of Amikacin in Pediatric Patients: A Comprehensive Review of Population Pharmacokinetic Analyses. Clin Pharmacokinet 57:1217–1228.

26. 2020. European Medicines Agency - EMEA/H/A-31/1476 - Article 31 referral assessment report of fosfomycin-containing medicinal products.

27. Brady M, Jackson M, Kimberlin D, Long S. 2018. Red book: 2018–2021 report of the committee on infectious diseases. 31st ed. American Academy of Pediatrics, Itasca.

559 28. EUCAST. 2020. The European Committee on Antimicrobial Susceptibility Testing.
560 Breakpoint tables for interpretation of MICs and zone diameters Version 10.0.

561 29. Bulitta JB, Hope WW, Eakin AE, Guina T, Tam VH, Louie A, Drusano GL, Hoover JL. 2019.
562 Generating Robust and Informative Nonclinical *In Vitro* and *In Vivo* Bacterial Infection
563 Model Efficacy Data To Support Translation to Humans. Antimicrob Agents Chemother
564 63:1–25.

565 30. Merino-Bohórquez V, Docobo-Pérez F, Sojo J, Morales I, Lupión C, Martín D, Cameán M,
566 Hope W, Pascual, Rodríguez-Baño J. 2018. Population pharmacokinetics and
567 pharmacodynamics of fosfomycin in non–critically ill patients with bacteremic urinary
568 infection caused by multidrug-resistant *Escherichia coli*. Clin Microbiol Infect 24:1177–
569 1183.

570 31. Docobo-Pérez F, Drusano GL, Johnson A, Goodwin J, Whalley S, Ramos-Martín V,
571 Ballestero-Tellez M, Rodriguez-Martinez JM, Conejo MC, Van Guilder M, Rodríguez-Baño
572 J, Pascual A, Hope WW. 2015. Pharmacodynamics of fosfomycin: Insights into clinical use
573 for antimicrobial resistance. Antimicrob Agents Chemother 59:5602–5610.

574 32. VanScoy BD, McCauley J, Ellis-Grosse EJ, Okusanya OO, Bhavnani SM, Forrest A, Ambrose
575 PG. 2015. Exploration of the pharmacokinetic-pharmacodynamic relationships for
576 fosfomycin efficacy using an in Vitro infection model. Antimicrob Agents Chemother
577 59:7170–7177.

578 33. Ramos-Martín V, Johnson A, Livermore J, McEntee L, Goodwin J, Whalley S, Docobo-
579 Pérez F, Felton TW, Zhao W, Jacqz-Aigrain E, Sharland M, Turner MA, Hope WW. 2016.

Pharmacodynamics of vancomycin for CoNS infection: Experimental basis for optimal use of vancomycin in neonates. J Antimicrob Chemother 71:992–1002.

34. Warn PA, Livermore J, Howard S, Felton TW, Sharp A, Gregson L, Goodwin J, Petraitiene R, Petraitis V, Cohen-Wolkowiez M, Walsh TJ, Benjamin DK, Hope WW. 2012. Anidulafungin for neonatal hematogenous Candida meningoencephalitis: Identification of candidate regimens for humans using a translational pharmacological approach. Antimicrob Agents Chemother 56:708–714.

35. Ramos-Martín V, Johnson A, McEntee L, Farrington N, Padmore K, Cojutti P, Pea F, Neely MN, Hope WW. 2017. Pharmacodynamics of teicoplanin against MRSA. J Antimicrob Chemother 72:3382–3389.

36. Kellogg JA, Ferrentino FL, Goodstein MH, Liss J, Shapiro SL, Bankert DA. 1997. Frequency of low level bacteremia in infants from birth to two months of age. Pediatr Infect Dis J 16:381–385.

37. Dietzman DE, Fischer GW, Schoenknecht FD. 1974. Neonatal *Escherichia coli* septicemia-bacterial counts in blood. J Pediatr 85:128–130.

38. Allegaert K, Scheers I, Adams E, Brajanoski G, Cossey V, Anderson BJ. 2008. Cerebrospinal fluid compartmental pharmacokinetics of amikacin in neonates. Antimicrob Agents Chemother 52:1934–1939.

39. Pfausler B. 2004. Concentrations of fosfomycin in the cerebrospinal fluid of neurointensive care patients with ventriculostomy-associated ventriculitis. J Antimicrob Chemother 53:848–852.

601 40. Amikacin 250 mg/ml Injection - Summary of Product Characteristics (SmPC) - (emc).

602 41. Fomicyt 40 mg/ml powder for solution for infusion - Summary of Product Characteristics
603 (SmPC) - (emc).

604 42. Winkler HH. 1973. Distribution of an inducible hexose phosphate transport system
605 among various bacteria. J Bacteriol 116:1079–1081.

606 43. 2003. Determination of minimum inhibitory concentrations (MICs) of antibacterial
607 agents by broth dilution. Clin Microbiol Infect 9:ix–xv.

608 44. D'Argenio DZ, Schumitzky A, Wang X. 2009. ADAPT 5 User's Guide:
609 Pharmacokinetic/Pharmacodynamic Systems Analysis Software. Biomed Simulations
610 Resour.

611 45. Viechtbauer W. 2010. Conducting meta-analyses in R with the metafor. J Stat Softw
612 36:1–48.

613 46. J.S. Cadwell J. 2012. The Hollow Fiber Infection Model for Antimicrobial
614 Pharmacodynamics and Pharmacokinetics. Adv Pharmacoepidemiol Drug Saf 01:1–5.

615 47. Hospira. 2015. Amikacin 250 mg/ml Injection SPC. medicines.org.uk.

616 48. Abdel-Hady E, El Hamamsy M, Hedaya M, Awad H. 2011. The efficacy and toxicity of two
617 dosing-regimens of amikacin in neonates with sepsis. J Clin Pharm Ther 36:45–52.

618 49. Allegaert K, Anderson BJ, Cossey V, Holford NHG. 2006. Limited predictability of amikacin
619 clearance in extreme premature neonates at birth. Br J Clin Pharmacol 61:39–48.

620 50. Hughes KM, Johnson PN, Anderson MP. 2017. Comparison of Amikacin Pharmacokinetics

621 in Neonates Following Implementation of a New Dosage Protocol. J Pediatr Pharmacol
622 Ther 22:33–40.

623 51. Howard JB, McCracken GH, Trujillo H, Mohs HE. 1976. Amikacin in newborn infants:
624 comparative pharmacology with kanamycin and clinical efficacy in 45 neonates with
625 bacterial diseases. Antimicrob Agents Chemother 10:205–210.

626 52. Kenyon CF, Knoppert DC, Lee SK, Vandenberghe HM, Chance GW. 1990. Amikacin
627 pharmacokinetics and suggested dosage modifications for the preterm infant.
628 Antimicrob Agents Chemother 34:265–268.

629 53. Blaser J. 1985. In-vitro model for simultaneous simulation of the serum kinetics of two
630 drugs with different half-lives. J Antimicrob Chemother 15:125–130.

631 54. Neely MN, Van Guilder MG, Yamada WM, Schumitzky A, Jelliffe RW. 2012. Accurate
632 detection of outliers and subpopulations with pmetrics, a nonparametric and parametric
633 pharmacometric modeling and simulation package for R. Ther Drug Monit 34:467–76.

634 55. Kane Z, Gastine S, Williams P, Berkley JA, Ellis S, Correia E, Darlow C, Hope W, Sharland
635 M, Standing JF. 2020. Abtract 4568: PK/PD of intravenous and oral fosfomycin in
636 neonates with presumed serious bacterial Infection. ECCMID Abstr B 2020 2206.

637 56. Illamola SM, Colom H, van Hasselt JGC. 2016. Evaluating renal function and age as
638 predictors of amikacin clearance in neonates: model-based analysis and optimal dosing
639 strategies. Br J Clin Pharmacol 793–805.

640

641 **Tables**

Bacterial species	Amikacin MIC (mg/L)										
	≤0.0625	**0.125**	**0.25**	**0.5**	**1**	**2**	**4**	**8**	**16**	**32**	**>32**
E. coli	-	-	-	-	-	1	3	2	3	1	-
K. pneumoniae	-	-	-	-	1	3	2	2	-	-	2
MRSA	-	-	-	-	-	4	3	-	-	-	3
S. agalactiae	-	-	-	-	-	-	-	-	1	1	8

642

Bacterial species	Fosfomycin MIC (mg/L)										
	≤0.0625	**0.125**	**0.25**	**0.5**	**1**	**2**	**4**	**8**	**16**	**32**	**>32**
E. coli	-	-	-	-	-	5	2	1	-	-	2
K. pneumoniae	-	-	-	-	-	-	1	-	-	1	8
MRSA	-	-	1	2	2	2	2	-	-	-	1
S. agalactiae	-	-	-	-	-	2	2	2	1	2	1

643 Tables 1a and 1b: Fosfomycin and amikacin MIC distributions in the neonatal sepsis bacterial

644 pathogen panel.

645

646

Parameter	Mean	Median	**95% Credibility interval**
V1 (L)	0.459	0.469	0.416 – 0.5
V2 (L)	0.359	0.312	0.306 – 0.417
Cl1 (L/h)	0.082	0.077	0.0755 – 0.0967
Cl2 (L/h)	0.038	0.031	0.0308 – 0.0369
Kgs	1.320	1.124	1.000 - 1.579
Kks	2.698	2.922	2.700 - 3.000
$E50_1s$ (mg/L)	9.081	6.805	4.417 – 11.260
$E50_2s$ (mg/L)	11.674	6.768	4.041 – 17.540
α_s	16.288	13.046	3.439 – 29.997
Kgr1	1.375	1.324	1.239 – 1.329
Kkr1	2.384	2.221	1.933 – 2.902
$E50_1r1$ (mg/L)	34.554	28.833	28.228 – 42.833
α_{r1}	17.023	20.520	11.021 – 22.068
Kgr2	1.361	1.367	1.299 – 1.375
Kkr2	2.325	2.070	1.972 – 2.872
$E50_2r2$ (mg/L)	37.795	39.150	28.819 – 43.860
α_{r2}	19.815	25.227	7.259 – 29.675
H1s	3.794	4.801	2.726 – 4.996
H2s	3.347	3.923	0.735 – 4.967

H1r1	2.160	2.488	1.205 – 2.831
H2r2	2.776	2.913	0.883 – 3.942

Table 2: Parameter values estimates with 95% credibility interval from HFIM PKPD model. V = Volume of distribution; C = clearance, Kg = bacterial growth constant; Kk = bacterial kill constant; E50 = Concentration of drug achieving 50% of efficacy; α = interaction parameter; H = Hill constant. Parameter suffices are defined as follows; 1 = relating to fosfomycin; 2 = relating to amikacin; s = relating to wildtype bacterial population; r1 = relating to 'fosfomycin resistant' bacterial population; r2 = relating to 'amikacin resistant' bacterial population.

Strain Number	Species	Resistance mechanisms	Amikacin MIC	Fosfomycin MIC
ST195	*E. coli*	CTX-M-14	4	1
I1057	*E. coli*	CTX-M-15, CMY-23, FQ-resistant	32	2
NCTC 13451	*E. coli*	CTX-M-15, OXA-1, TEM-1, aac6'-Ib-cr, mph(A), catB4, tet(A), dfrA7, aadA5, sulI	16	4
BAA2523	*E. coli*	OXA-48	4	8
L75546	*K. pneumoniae*	NS	64	4
1237221	*K. pneumoniae*	SHV-OSBL, CTX-M-15	8	32
1216477	*K. pneumoniae*	SHV-OSBL, TEM-OSBL, CTX-M-15	8	32
NCTC 13438	*K. pneumoniae*	KPC3	32	32
1256506	*K. pneumoniae*	SHV-OSBL; TEM-OSBL; CTX-M-2; CMY-2	2	128
L41464	*K. pneumoniae*	NS	16	128

654

655 Table 3: Details of strains used in HFIM testing physiological pharmacokinetics of

656 fosfomycin/amikacin. NS = not sequenced, at time of writing.

		Amikacin MIC (mg/L)								
		1	**2**	**4**	**8**	**16**	**32**	**64**	**128**	**256**
Fosfomycin MIC (mg/L)	**256**	91.33%	51.81%	3.43%	0.00%	0.00%	0.00%	0.00%	0.00%	0.00%
	128	99.42%	91.33%	51.81%	3.43%	0.00%	0.00%	0.00%	0.00%	0.00%
	64	99.97%	99.42%	91.33%	51.81%	3.43%	0.00%	0.00%	0.00%	0.00%
	32	100.00%	99.97%	99.42%	91.33%	51.81%	3.43%	0.00%	0.00%	0.00%
	16	100.00%	100.00%	99.97%	99.42%	91.33%	51.81%	3.43%	0.00%	0.00%
	8	100.00%	100.00%	100.00%	99.97%	99.42%	91.33%	51.81%	3.43%	0.00%
	4	100.00%	100.00%	100.00%	100.00%	99.97%	99.42%	91.33%	51.81%	3.43%
	2	100.00%	100.00%	100.00%	100.00%	100.00%	99.97%	99.42%	91.33%	51.81%
	1	100.00%	100.00%	100.00%	100.00%	100.00%	100.00%	99.97%	99.42%	91.33%

Table 4: Probability of attainment of the target $(fAUC_F/\ MIC_F) * (fAUC_A/\ MIC_A)\ > 2709.5$ across a range of amikacin and fosfomycin MICs using 10,000 Monte Carlo simulated neonatal amikacin and fosfomycin *f*AUCs. Grey shading denotes MIC combinations with probability of target attainment < 95%.

Figures

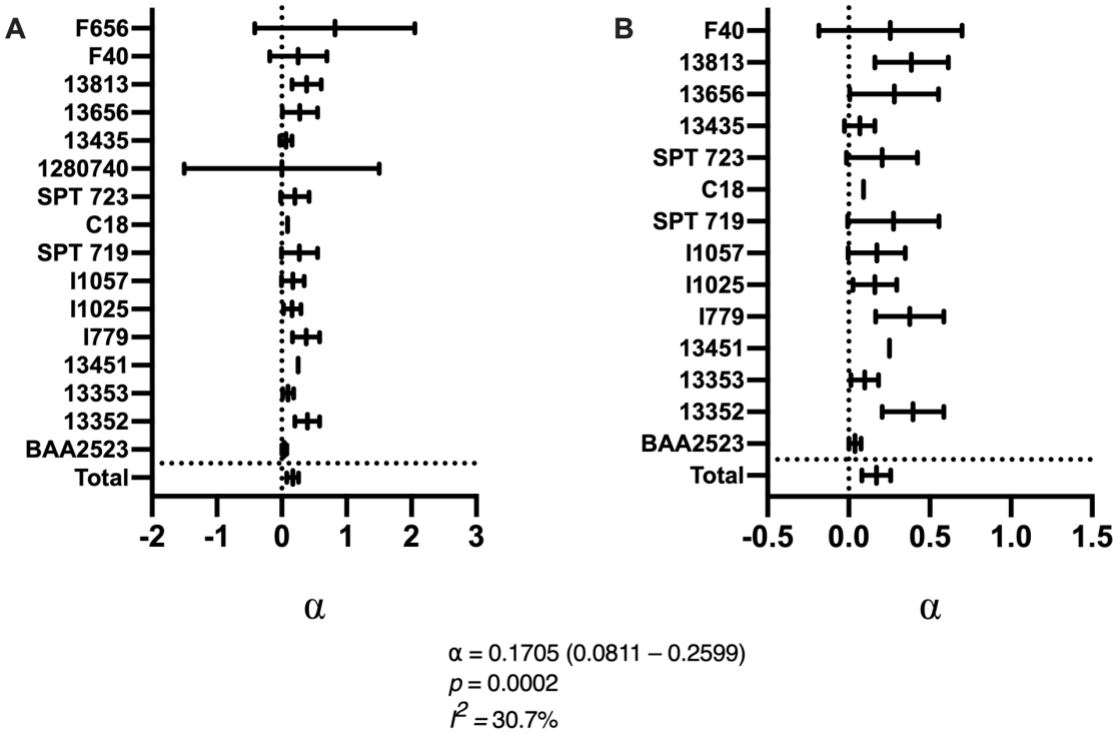

Figure 1– Modelled output for checkerboard assays to three antimicrobial combinations against 16 isolates, with a combined total statistic for each combination. Figure 1a details full results of all strains; Figure 1b shows the same data with the two isolates with wide CI intervals censored (the total statistic is unchanged and still includes data from these isolates). α is the interaction parameter in the Greco model indicating the level of synergy. A confidence interval (CI) >0 indicates presence of synergy; CI <0 indicates antagonism; a CI containing 0 indicates no interaction with additive effects only. α and p values for combined statistic are given below the figures. I^2 represents the heterogeneity in effect between individual strains.

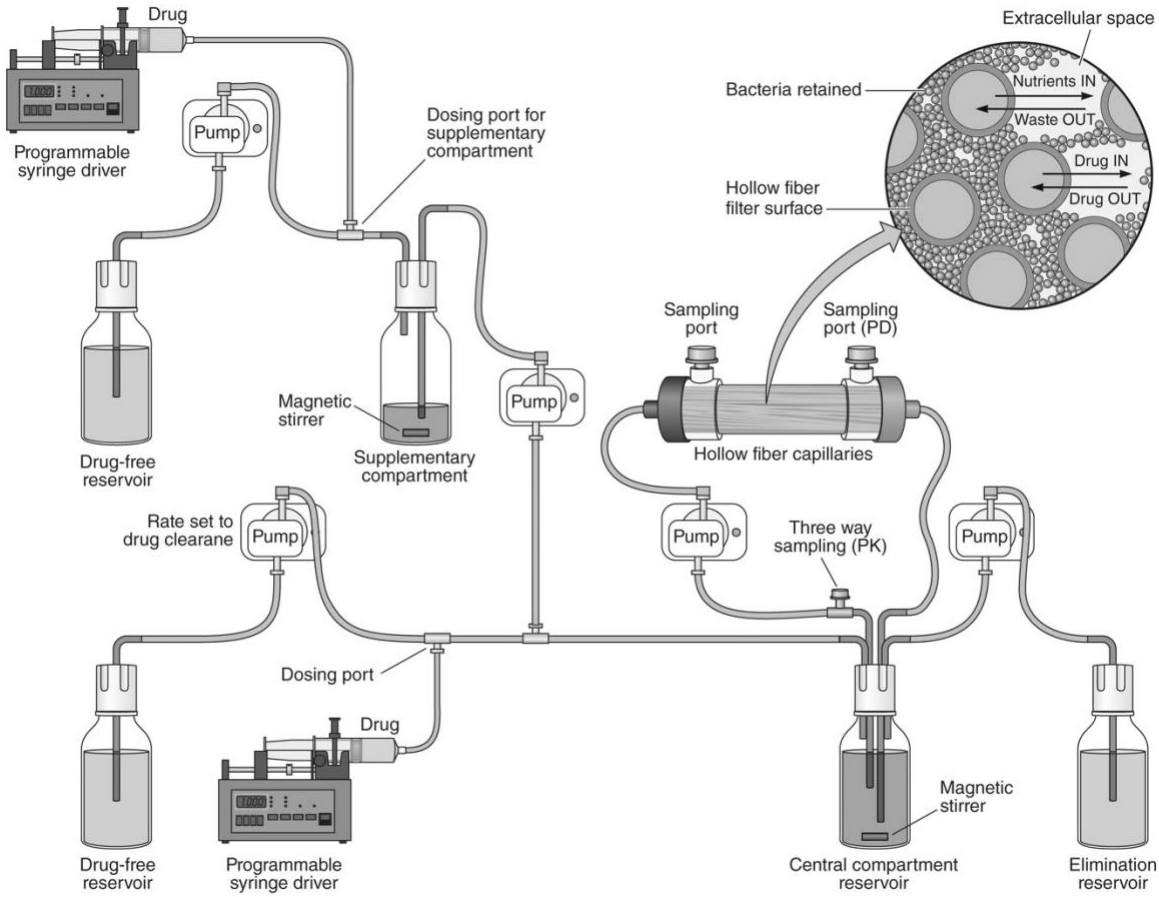

671

672 Figure 2 – Schematic setup of HFIM for combination antimicrobials. For arms with a single drug

673 administered, the supplementary compartments were omitted.

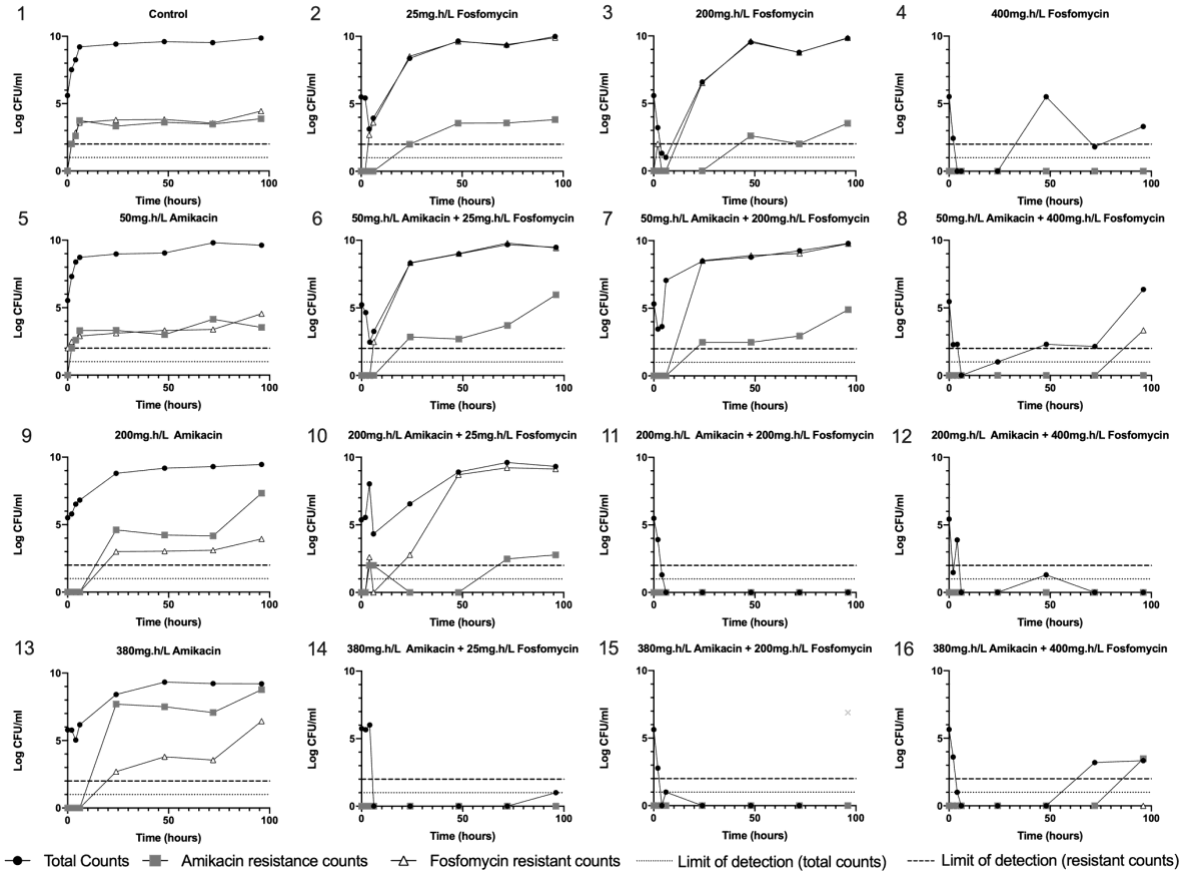

Figure 3 – Pharmacodynamic output of 16-arm fosfomycin/amikacin combination HFIM experiment, with labelled *f*AUC$_{0\text{-}24}$ for each arm. Grey cross in arm 15 was a real data-point in the initial experiment but was not reproducible in repeat experiments. It is demonstrated here for completeness but was not included in the modelling.

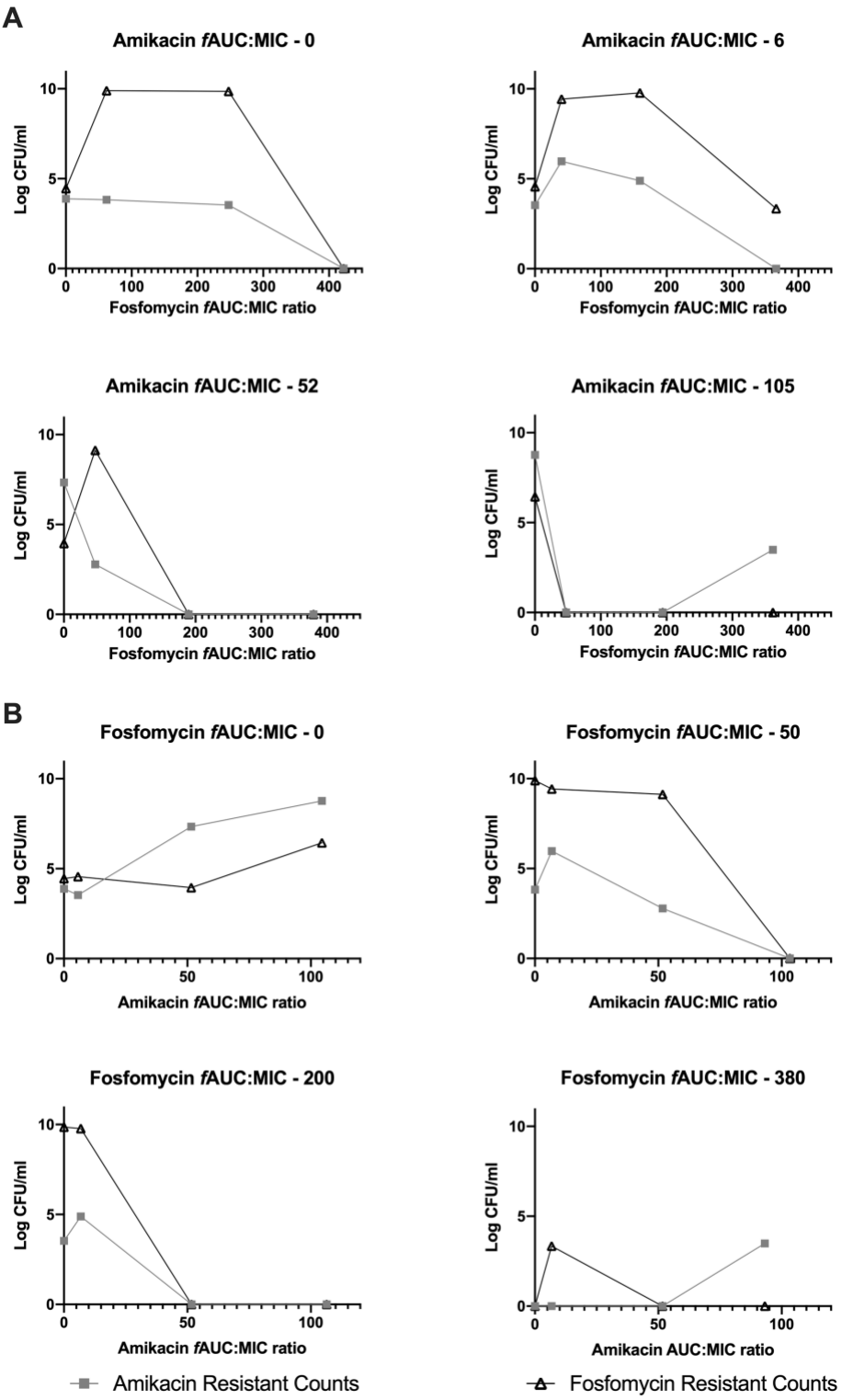

Figure 4 – Pharmacodynamic relationships of emergence of resistance in relation to modelled *f*AUC:MIC ratios for each agent. (A) Increasing fosfomycin *f*AUC:MIC on a background of fixed

683 Amikacin *f*AUC:MIC; (B) Increasing amikacin *f*AUC:MIC on a background of fixed fosfomycin

684 *f*AUC:MIC.

685

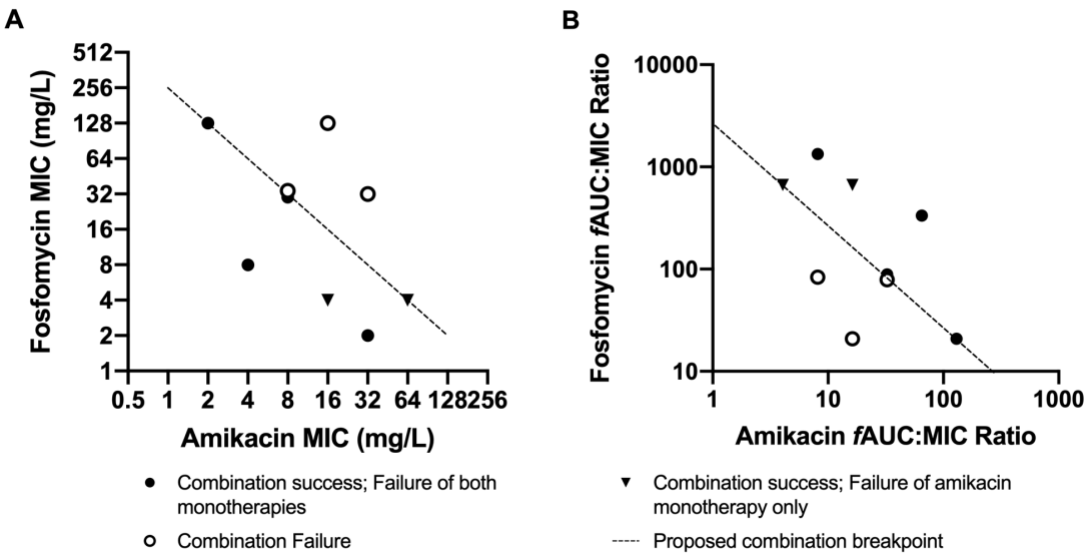

686

687 Figure 5 – Summary of pharmacodynamic outputs of fosfomycin/amikacin antimicrobial

688 combination and monotherapy regimens in HFIM shown by pathogen fosfomycin/amikacin

689 MICs (A) and fosfomycin/amikacin *f*AUC:MIC ratio (B). Success is defined by bacterial kill to

690 sterility at the end of the experiment.